Digestive Diseases and Sciences, Vol. 51, No. 7 (July 2006), pp. 1260–1268 (© 2006)
DOI: 10.1007/s10620-006-8046-3

Investigation of Musashi-1 Expressing Cells in the Murine Model of Dextran Sodium Sulfate-Induced Colitis

TADAHISA FUKUI, MD, HIROAKI TAKEDA, MD, HONG-JIN SHU, MD, KATSUYOSHI ISHIHAMA, MD, SAYAKA OTAKE, MD, YASUKUNI SUZUKI, MD, SHOICHI NISHISE, MD, NANAMI ITO, MD, TAKESHI SATO, MD, HITOSHI TOGASHI, MD, and SUMIO KAWATA, MD

Musashi-1 (Msi-1), an RNA-binding protein, had been proposed to be a specific marker for neural stem/precursor cells. Msi-1 expressing cells in the intestinal epithelium are also strongly considered as potential stem/precursor cells. To clarify the behavior of those cells in the injury or regeneration phase, we investigated Msi-1 expressing cells of intestinal mucosa in the murine model of dextran sodium sulfate (DSS)-induced colitis. Immunohistochemically, Msi-1-positive cells were found in the area just along the layer of Paneth's cells in the small intestine and in the bottom layer of crypts in the large intestine. During DSS administration, the number of PCNA-positive cells in the large intestine increased markedly. In contrast, the number of Msi-1-positive cells decreased slightly with DSS but returned to normal after DSS administration was stopped. The level of mRNA for Msi-1 was consistent with the result of immunohistochemical examinations. Conclusively, we could describe the behavior of intestinal stem/precursor cells during inflammation using Msi-1.

KEY WORDS: Musashi-1; intestinal stem cell; dextran sodium sulfate; mouse; colitis.

Stem cells play roles in mucosal cell homeostasis and repair (1). Potten *et al.* have reported the location and characteristics of stem cells in the gastrointestinal epithelium (2–4). However, specific markers for stem cells in the intestine have not been elucidated. Okano and his colleagues have reported that Msi-1 is a marker for neural stem cells (5). In *Drosophila*, Msi-1 controls cell differentiation in external sensory organs through regulation of the activity of the Numb protein during development (5–8). It has also been reported in mice and humans that Msi-1 can be used as a marker for neural stem cells in embryos as well as in adults (9, 10). In addition, our group showed that Msi-1 is expressed in the hepatic cells of embryos (11).

Recently, Msi-1 had been reported as a strong candidate maker for intestinal stem/precursor cells. Kayahara *et al.* (12) described Msi-1-positive cells in the mouse small intestine, and Nishimura *et al.* (13) did in the human colon. The location of intestinal stem/precursor cells has been revealed, but the behavior of those cells in inflamed epithelium has not been precisely analyzed. In this study, we immunohistochemically detected Msi-1-positive cells in mouse intestinal epithelium and investigated the behavior of Msi-1 expressing cells in the colonic mucosa damaged by administration of dextran sodium sulfate (DSS).

Manuscript received July 24, 2005; accepted July 27, 2005

From the Department of Gastroenterology, Yamagata University School of Medicine, Yamagata, Japan.

This work received financial support from 21st Century Center of Excellence Program of the Japan Society for the Promotion of Science Grant-in-Aid F-1 and Ministry of Education, Science, and Culture in Japan Grant-in-Aid 16046202.

Address for reprints requests: Hiroaki Takeda, MD, Department of Gastroenterology, Yamagata University School of Medicine, 2-2-2 Iida-Nishi, Yamagata, Japan, 990-9585; htakeda@med.id.yamagata-u.ac.jp.

METHODS

Animals. Pregnant BALB/c mice at day 12.5 were purchased from CLEA Japan (Tokyo) and sacrificed at day 17.5. Anesthesia was carried out by intraperitoneal injection of pentobarbital, 30–40 mg/kg body weight, after inhalation of diethyl ether. Embryos were taken out through an abdominal incision, immersed in 10% (v/v) buffered formalin for 1 day, and embedded in paraffin after a vertical incision was made at their center. Adult female mice, 20 g in body weight, were similarly anesthetized with diethyl ether and pentobarbital, and the small and large intestines were collected and immersed in cold saline. The proximal one-third of the total length of the small intestine, representing the jejunum, was dissected into four portions, each of which was 0.5 cm long, and then fixed with 10% buffered formalin. The total length of the large intestine was also dissected into four portions, each of which was 0.5 cm long, and was fixed with 10% buffered formalin. The formalin-fixed specimens were embedded in paraffin in such a way that the intestine could later be sliced longitudinally along its long axis. The rest of the small and large intestine was placed on glass on ice, and its muscles and serosa were quickly removed. The remaining mucosa was frozen in liquid nitrogen to extract RNA.

DSS-Induced Colitis Model. To observe the intestinal mucosaduring mucosal inflammation and repair, colitis was induced in female BALB/c mice of ∼20-g body weight by oral administration of 5% (w/v) DSS (MW ∼54,000, 19.1% S content; Meito Sangyo, Tokyo) in drinking water (14). DSS was administered for 5 days. Specimens of the small and large intestines were collected at day 5 (DSS[+]). As controls, specimens of the intestine from mice not given DSS were also examined (CR). After the administration, specimens of the intestine were obtained at day 3 (day 3[–]), day 7 (day 7[–]), and day 14 (day 14[–]). Anesthesia, specimen collection, and fixation were carried out as described above for normal adult mice. Specimens of the intestine from 14 mice were collected for hematoxylin–eosin staining, and specimens from 8 of the 14 mice were also used for immunostaining. Mucosa was also prepared as described above for normal adult mice in order to extract RNA. The severity of DSS colitis was evaluated on the basis of the histologic colitis scoring method developed by Williams *et al.* (14).

Immunohistochemistry. Sliced specimens embedded in paraffin, 4 μm thick, were stained with anti-Msi-1 antibody using ABC kits (Vector Laboratories, Burlingame, CA). After the paraffin was removed, the sliced specimens were immersed in methanol containing 0.3% (v/v) H_2O_2 for 30 min to inactivate intrinsic peroxidase and were then heated in 0.01 M citric acid buffer, pH 6.0, for 20 min using an 800-W microwave. The slices were blocked in skim milk for 10 min and then probed with rat anti-Msi-1 monoclonal antibody (1:5000 dilution; a gift from Prof. Okano, Keio University, Tokyo) overnight at 4°C. The slices were then washed with PBS, incubated with biotinylated rabbit anti-rat antibody (Vectastain ABC Elite; Vector Laboratories) for 120 min, washed again with PBS, incubated with avidin-conjugated peroxidase (Vectastain ABC Elite) for 30 min, and then incubated with DAB for 3 min in a dark room. The specimens were incubated with hematoxylin for nuclear staining, dehydrated with ethanol, and then sealed with Entellan after washing with xylene. The tissues were also stained with a PCNA kit (DAKO Japan, Tokyo) and with rabbit anti-chromogranin-A and -B polyclonal antibodies (1:100 dilution; PROGEN Biotechnik, Heidelberg, Germany) using ABC kits (Vectastain ABC Elite).

Msi-1 mRNA Expression. For total RNA extraction, Isogen kits (Wako Pure Chemical Industries, Tokyo) were used. Mucosa from the small or large intestine, 50–100 mg, was homogenized with 1 ml of Isogen solution. After centrifugation at 12,000*g* for 15 min at 4°C, supernatant was mixed with 0.5 ml of isopropanol and kept for 10 min at room temperature. After centrifugation at 12,000*g* for 15 min at 4°C, the supernatant was mixed with 1 ml of 75% (v/v) aqueous ethanol. The pellets collected by centrifugation at 7500*g* for 5 min at 4°C were dried under vacuum, dissolved in DEPC-treated H_2O, and then heated for 15 min at 60°C.

The total RNA prepared above was annealed with random hexamers (Life Technologies, Rockville, MD) by heating for 10 min at 70°C followed by cooling in ice. To the annealed solution, fivefold concentrated reverse transcription buffer (Life Technologies), dNTP mixtures, and DTT were added, and the mixture was incubated for 5 min at 25°C. MMLV reverse transcriptase (Life Technologies) was added to the mixture, which was then sequentially incubated for 10 min at 25°C, for 50 min at 42°C, and for 15 min at 70°C. The reaction was terminated by placing the reaction tubes on ice.

To detect Msi-1 mRNA, nested polymerase chain reaction (PCR) was performed using the following oligonucleotide primers designed from the human Msi-1 nucleotide sequence deposited in the DDBJ GenBank (accession no. AB012851): outside primers, 5′-GTA CCC ATT GGT GAA GGC TGT GGC A-3′ (sense strand) and 5′-CAA GAT GTT CAT CGG GGG ACT CAG TT-3′ (antisense strand); and inside primers, 5′-GGC TTC GTC ACT TTC ATG GAC CAG GCG-3′ (sense strand) and 5′-GGG AAC TGG TAG GTG TAA C-3′ (antisense strand). As a positive control, ß-actin mRNA was also amplified by RT-PCR using the primers 5′-GTC GAC AAC GGC TCC GGC ATG TGC A-3′ (sense strand) and 5'-GGA TCT TCA TGA GGT AGT CAG TCA G-3′ (antisense strand) (15). Using the synthesized cDNA as template, PCR was carried out in PCR buffer (TAKARA BIO, Shiga, Japan) containing dNTPs, primers, and Taq DNA polymerase (TAKARA BIO). Using the outside primers, Msi-1 cDNA was amplified through 40 reaction cycles, each of which consisted of incubation for 1 min at 94°C, for 2 min at 58°C, and for 1 min at 72°C, followed by a final extension reaction for 7 min at 72°C. Using the resulting PCR products as templates, the same reaction conditions were used for PCR using the inside primers. ß-Actin mRNA was detected by 30 cycles of PCR, each of which consisted of incubation for 1 min at 94°C, for 2 min at 58°C, and for 1 min at 72°C, followed by a final extension for 7 min at 72°C. The PCR products were observed under a UV lamp after separation by 3% agarose gel electrophoresis and staining with 0.5 μg/ml ethidium bromide for 30 min.

Statistical Analysis. Data are expressed as the mean ± SD. Friedman's test and Mann-Whitney's *U*-test were used for statistical analysis of data, and differences with $P < 0.05$ were considered to be statistically significant.

RESULTS

Msi-1-Positive Cells in the Intestine of Embryonic Mice

As a positive control, the neural cells in the spinal cord and the area surrounding the cerebral ventricle of day 17.5

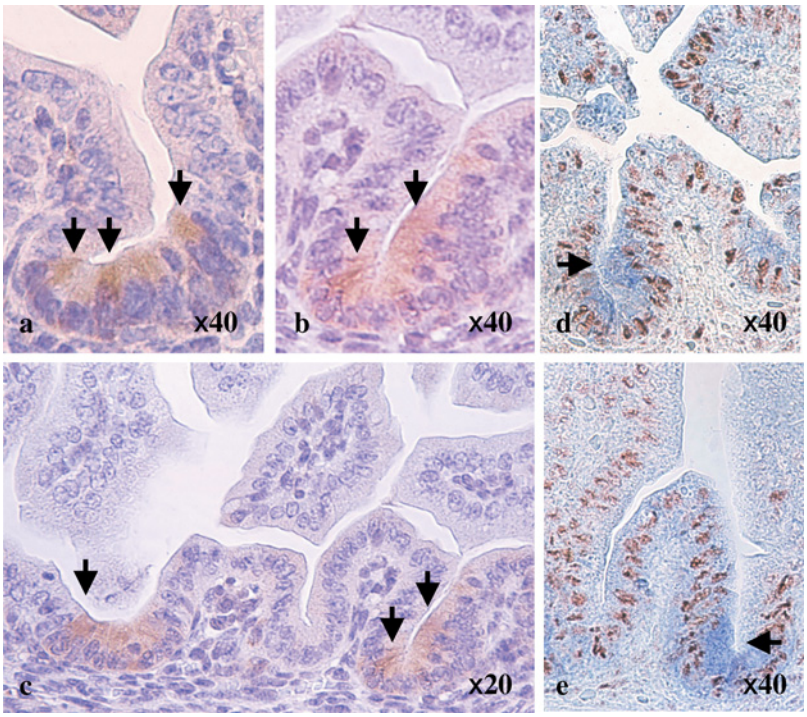

Fig 1. Msi-1-positive cells in the intestine of embryonic mice at day 17.5. (a–c) Msi-1-positive cell in the intestine. Note that the positive cells shown by arrows were present in a portion of the crypts but not in the villi. (c, d) Double staining with anti-Msi-1 and anti-PCNA antibodies. Note that there is no proper proliferative zone in the intestinal crypts of embryonic mice and that most of the cells in the intestinal epithelium are positive to anti-PCNA antibody and a fraction of cells at the bottom of crypts is stained with anti-Msi-1 antibody, as shown by arrows.

embryos were successfully stained with anti-Msi-1 antibody. In the same slides, Msi-1-positive cells were also observed in the intestinal epithelium (Figures 1a–c). The multiple cells stained were observed in crypts but not in villi. On the other hand, almost all the cells of the mucosal epithelium were positively stained by immunostaining with anti-PCNA antibody (Figures 1d and e).

Msi-1-Positive Cells in the Intestine of Adult Mice

Localization of Msi-1-Positive Cells in the Small Intestine. Several Msi-1 expressing cells were observed in the bottom area of the crypt in the small intestinal epithelium. Msi-1 was positive in the cytoplasm, but not in the nucleus. Paneth's cells were Msi-1-negative. Cells of which the cytoplasm was most strongly stained were present in the upper layers. No positive cells were observed in the upper end of crypts or in villi. In the small intestine, the mean number of Msi-1-positive cells per crypt was 6.1 ± 0.41 (range, 3 to 14) (Figures 2 and 3a).

Localization of Msi-1-Positive Cells in the Large Intestine. A markedly smaller number of positive cells was observed in the large intestine than in the small intestine. Not all crypts contained Msi-1-positive cells. Even in the positive crypts, only one or two Msi-1-positive cells were present at the bottom cell layers. The mean number of Msi-1-positive cells per crypt was 0.21 ± 0.41

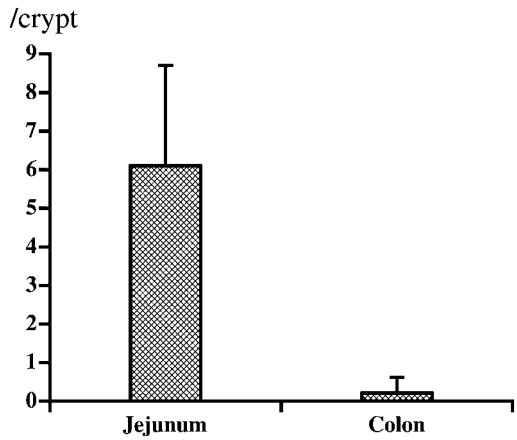

Fig 2. Number of Msi-1-positive cells in the normal intestine of embryonic mice.The numbers of Msi-1-positive cells in the small and large intestine were 6.1 ± 2.6/crypt ($n = 8$) and 0.21 ± 0.41/crypt ($n = 8$), respectively. Note the clear difference in the number of positive cells.

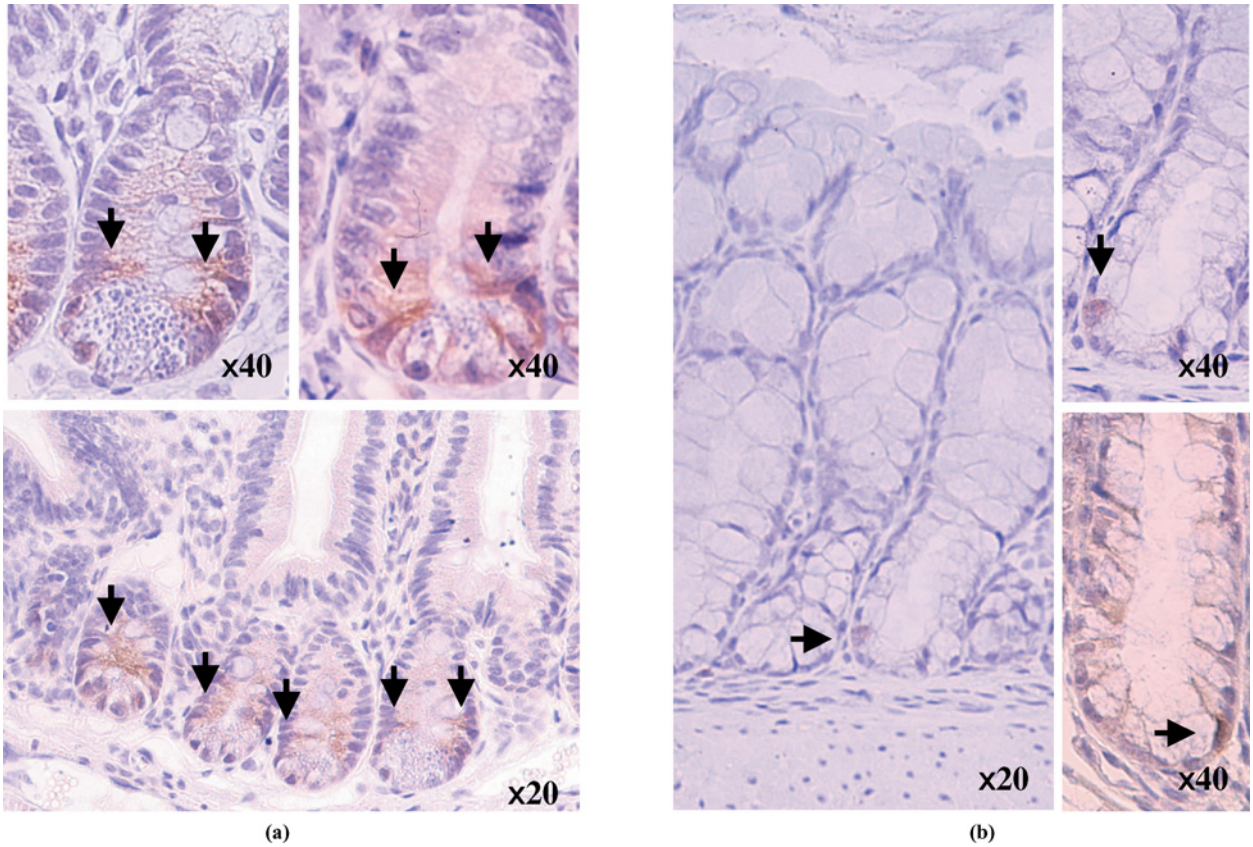

Fig 3. Immunohistological staining of the intestine from adult mice with anti-Msi-1 antibody. (a) Msi-1-positive cells in the small intestine. Note the positive cells right or just above Paneth's cells. (b) Msi-1-positive cells in the large intestine. Note the positive cells at the bottom of crypts as a result of the lack of Paneth's cells.

(range, 0 to 2) (Figures 2 and 3b). Double staining with anti-chromogranin-A/B antibodies and with anti-Msi-1 antibody revealed that the Msi-1-positive cells were clearly different from chromogranin-A/B-positive cells (Figure 4).

Detection of Msi-1 mRNA Expression in the Intestine of Adult Mice

By nested PCR, expression of Msi-1 mRNA was detected in both the small and the large intestinal epithelia (Figure 5). The expression level of mRNA in the small intestine was higher than that in the large intestine. This is consistent with the results observed by immunohistochemical staining.

Msi-1-Positive Cells in DSS-Induced Colitis

Histologic Colitis Scoring Model. On the basis of the histologic colitis scoring method (14), scores of DSS-induced colitis were as follows: 19.2 ± 1.3 at day 5 (DSS[+]), 16.1 ± 1.3 at day 3 after halting DSS administration (day 3[–]), 9.7 ± 2.0 at day 7(–), and 11.4 ± 1.2 at day 14(–). The highest score was observed during DSS administration, and the scores gradually decreased after DSS was discontinued (Figure 6). In the small intestine, the numbers of Msi-1- or PCNA-positive cells in mice with colitis were not significantly different from those in control mice. By double staining with anti-Msi-1 and anti-PCNA antibodies, Msi-1-positive cells were present in deeper cell layers than those where PCNA-positive cells resided (Figure 7). However, Msi-1-positive cells existed within the range of PCNA-positive cells.

Msi-1- and PCNA-Positive Cells in DSS-Induced Colitis. The number of Msi-1-positive cells was 0.29 ± 0.48/crypt in the control (CR), 0.067 ± 0.25/crypt at DSS(+), 0.23 ± 0.47/crypt at day 3(−), 0.31 ± 0.52/crypt at day 7(−), and 0.26 ± 0.46/crypt at day 14(−). Compared with the control, the number of Msi-1-positive cells decreased significantly during administration of DSS (DSS[+]). However, the number of Msi-1-positive cells returned to the control level by 3 days after stopping DSS administration

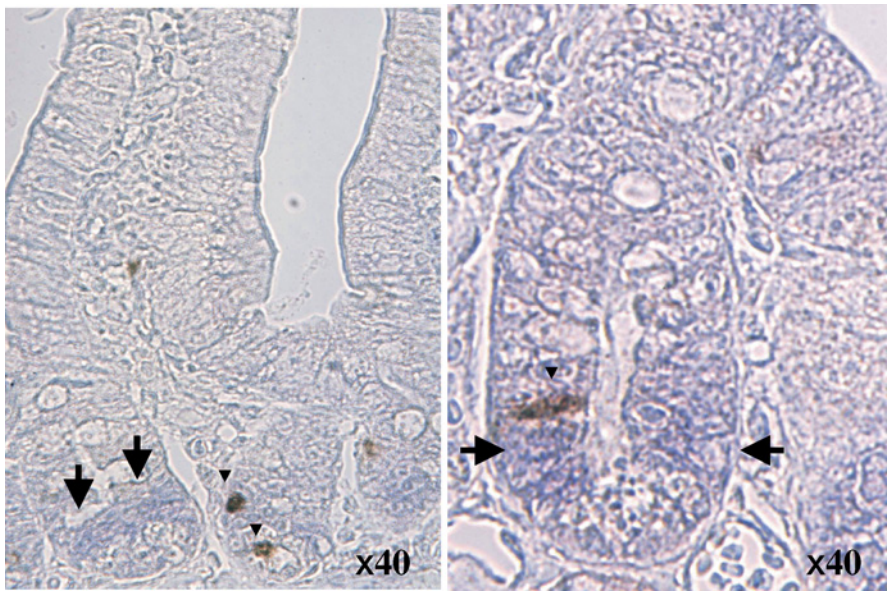

Fig 4. Immunohistological staining of the intestine with anti-Msi-1 and anti-chromogranin-A and -B antibodies.Msi-1-positive cells (arrow) and chromogranin-A- and -B-positive cells (arrowhead). Note that the two antibodies stained different cell types. Msi-1-positive cells and chromogranin-positive cells are clearly different.

(Figure 8a). The number of PCNA-positive cells was 8.1 ± 3.2/crypt in the control (CR), 16.4 ± 3.5/crypt at DSS(+), 14.9 ± 6.9/crypt at day 3(−), 6.7 ± 3.0/crypt at day 7(–), and 8.9 ± 4.0/crypt at day 14(−). The number of PCNA-positive cells was significantly increased by DSS administration and remained increased at 3 days after stopping DSS, but a significant difference was not observed at day 7(−) compared with the control (Figure 8b). These results indicate that Msi-1-positive and PCNA-positive cells behave differently during DSS-induced colitis and mucosal repair.

Msi-1 mRNA in DSS-Induced Colitis. Nested PCR was used to detect Msi-1 mRNA in the large intestine of mice with DSS-induced colitis. A cDNA fragment, 542 bp long, corresponding to Msi-1 mRNA was amplified from RNA prepared from the intestine during and after DSS administration. The expression level of Msi-1 mRNA decreased in the intestine with mucosal lesions, and the expression level returned to normal after administration of DSS was halted (Figure 9). This result is consistent with the observation that the number of Msi-1-positive cells decreased during the administration of DSS.

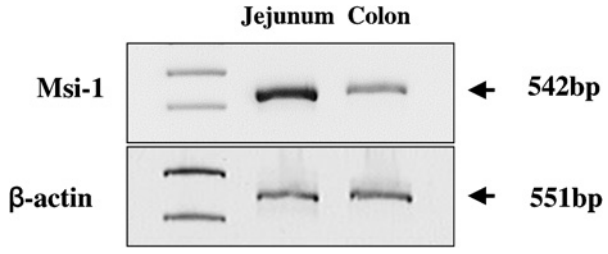

Fig 5. Detection of Msi-1 mRNA in the intestine of normal adult mice. Nested PCR was used to detect cDNA, 542 bp in size, corresponding to Msi-1 mRNA. RT-PCR was used to detect cDNA, 551 bp in length, derived from β-actin mRNA as a positive control.

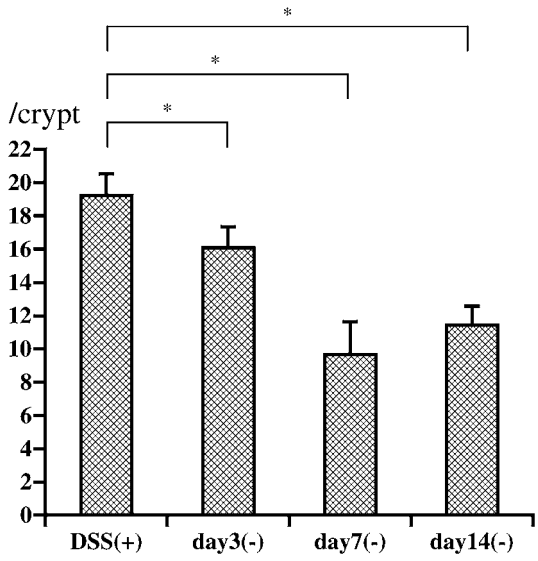

Fig 6. Histologic score of DSS-induced colitis. Histologic scores were significantly decreased at all stages examined ($n = 14$; $^*P < 0.05$).

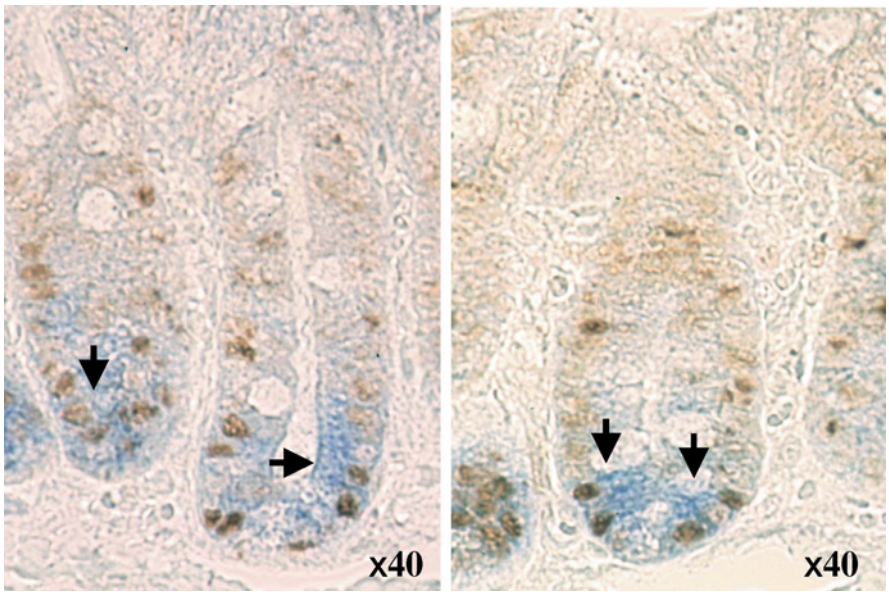

Fig 7. Double staining of the small intestine with anti-Msi-1 and anti-PCNA antibodies. When the entire cell layers of crypts were observed, Msi-1-positive cells were localized in the bottom cell layers. In contrast, most of the PCNA-positive cells were localized in the proliferative zone.

DISCUSSION

Studies on neural stem cells have recently become popular, and Msi-1, an RNA-binding protein, has been demonstrated by Okano and his colleagues to be a specific marker for neural precursor cells, including stem cells (5, 16, 17). The neural stem/precursor cells reside in area surrounding the ventricle and spinal cord of embryonic and adult mice (9, 18). The Notch signaling pathway regulates asymmetric cell division of the stem/precursor cells (19–28), and the Msi-1 protein is involved in this pathway by interacting with the Numb protein (29–31). Numb regulates Notch receptor activity through binding to the intracellular domain of Notch (32, 33). *Drosophila* lacking Msi-1 have a defect

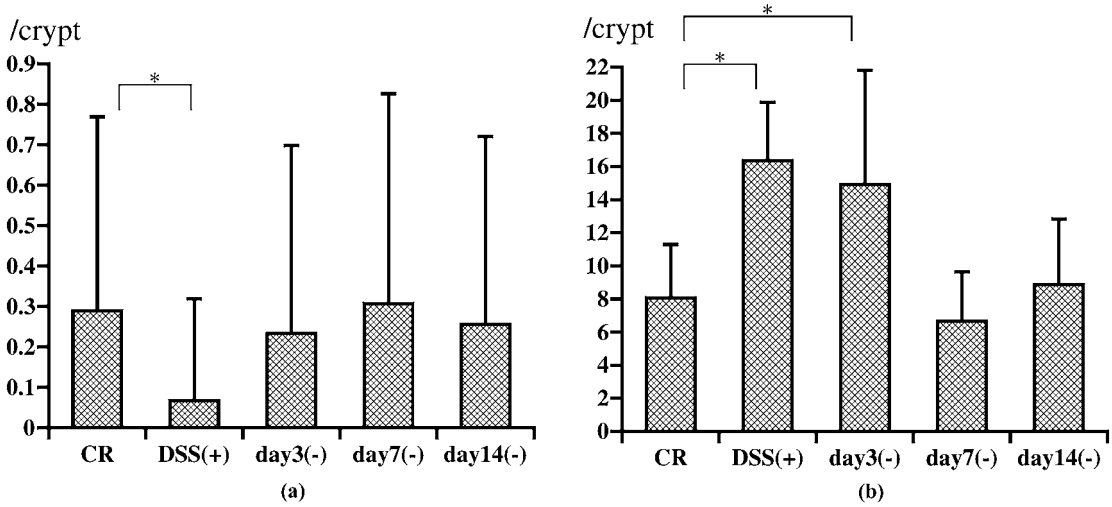

Fig 8. Numbers of Msi-1- or PCNA-positive cells in the intestine of mice with DSS-induced colitis. (a) The number of Msi-1-positive cells ($n = 8$; $*P < 0.05$). Note that there is no statistically significant difference in the number of positive cells at all colitis stages, even during mucosal healing, except for DSS(+). (b) The number of PCNA-positive cells ($n = 8$; $*P < 0.05$). Note that the number of positive cells is statistically significantly increased at DSS(+) and day 3(−) but returns to the normal level at day 14 (−).

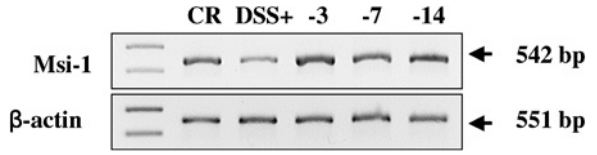

Fig 9. Detection of Msi-1 mRNA in the intestine of mice with DSS-induced colitis. Msi-1 mRNA was detected by nested PCR, as described under Materials and Methods, in the intestine of mice during the development of the lesion as well as during healing of the lesion after stopping administration of DSS. RT-PCR of β-actin mRNA is also shown as a positive control.

in differentiation of external sense organs such as hair and socket cells (5, 6). It is thought that Msi-1 also plays a role in asymmetric cell division, since the protein functions in the upstream process of Numb (29, 31). Kaneko *et al.* have reported that cultured neural stem cells are Msi-1-positive but that fully differentiated neurons are negative (9). Thus, Msi-1 seems to function in the asymmetric cell division of neural stem/precursor cells and can be used as a specific marker for these cells.

Stem cells are indispensable for the mucosal repair of the gastrointestinal tract and play important roles in mucosal homeostasis (34). Numerous studies on cell renewal and mucosal repair in the gastrointestinal tract have been published previously (35–39). Through asymmetric cell division, stem cells in the gastrointestinal epithelium produce precursor cells that differentiate into Paneth's, epithelial, neuroendocrine, and goblet cells (4, 41). It is thought that there is a proliferative zone at the bottom of crypts where cells divide asymmetrically or symmetrically and form cell layers (2). By observing proliferating cells in crypts after ionizing radiation, Potten *et al.* have reported the cell positions of the stem cells that are present (41, 42). They have also reported that Paneth's cells exist in the bottom three cell layers, that stem cells occupy the fourth layer, and that precursor cells occupy the fifth through seventh layers in crypts. In crypts of the large intestine, stem cells are present in the bottom cell layers because of the absence of Paneth's cells.

It has become apparent that every crypt cell is derived from a single stem cell. Furthermore, by observing crypts deficient in glucose-6-phosphate dehydrogenase because of gene mutation, Griffith *et al.* have found that all the cells of a crypt derive from a single stem cell through monoclonal cell proliferation (43, 44). Since all the cells in the gastrointestinal epithelium, particularly in the small intestine, are renewed in a very short time, 3–5 days, it is thought that precursor cells, not stem cells, in the proliferative zone produce a large number of mature cells in a short time. Indeed, Potten *et al.* have proposed that the proliferative zone has a pyramid-like structure, consisting of various cell layers with stem cells on top, and that the number of stem cells produced through asymmetric cell division is very small (2).

In the present study, we first verified that Msi-1-positive cells are found in the intestine of mice and these cells occupy positions similar to those where Potten *et al.* have proposed stem cells to reside (4). We used brain and intestine of embryonic mice as positive controls for careful investigation. Then, on double staining with anti-Msi-1 and anti-chromogranin-A and -B antibodies, it appeared that the Msi-1-positive cells are not neuroendocrine cells. Comparing small and large intestine, the mean number of cells expressing Msi-1 in the large intestine was 0.21 per crypt, much lower than in the small intestine. This is presumably due to the slower turnover of cells in the large intestine compared with the small intestine. We could not find Msi-1 expressing cells in every crypt. If we were able to observe isolated whole crypts by confocal laser microscopy, every crypt would have Msi-1-positive cells in the bottom area. Nishimura et al. (13) described 19.0 ± 7.53 Msi-1-positive cells per crypt of human colon.

Activated cell division in the intestine has previously been observed during mucosal repair (45). In our study, the number of PCNA-positive cells increased significantly during DSS-induced inflammation and, thereafter, returned to normal. This behavior of PCNA-positive cells is consistent with their roles in reproducing epithelial cells during the process of mucosal repair. In contrast, the number of Msi-1-positive cells temporarily decreased during DSS-induced inflammation, and then returned to levels similar to the control after DSS administration stopped. This indicates that, unlike PCNA-positive cells, Msi-1-positive cells do not proliferate during inflammation and the recovery phase. If the Msi-1-positive cells were stem cells and/or their close relatives, it would be reasonable that these cells would halt cell division to minimize gene mutations and chromosomal rearrangement during severe inflammatory mucosal damage. Instead, matured proliferating cells may quickly produce numerous epithelial cells to repair the mucosal injury. This may be an asymmetric and PCNA-positive process. As previously proposed (46), the cell reproduction system may have a pyramid-like structure, with ancestor stem cells on top, and may consist of cell layers in which precursor cells occupy several layers. It is thought that cells more mature than precursor cells may be responsible for the production of epithelial cells for repair processes in colitis.

Lower doses of radiation cause apoptosis of smaller numbers of cells of many types, including mature cells, than do higher doses. It has been reported that lower doses of radiation cause apoptosis of cells located in layers above those where Paneth's cells reside, in an area where stem

cells seem to be located (47, 48). Furthermore, although continuous administration of a carcinogenic agent, 1,2-dimethylhydrazine, induces cell proliferation, it also induces apoptosis of cells in the proliferative zone as well as at the bottom of crypts (49–51). Thus, minor lesions of the intestine induce apoptosis of stem/precursor cells, which may be a self-protecting mechanism that prevents production of tumor cells by DNA damage. It is, therefore, reasonable that the Msi-1-positive cells detected in this study may indeed be intestinal stem/precursor cells and that DSS-induced colitis may induce apoptosis of these Msi-1-positive cells. Further investigation is under way in our laboratory.

Msi-1-positive cells were localized at the place in the intestine where stem/precursor cells have previously been proposed to reside. In the DSS-induced colitis model, the number of PCNA-positive cells increased and the number of Msi-1-positive cells temporarily decreased during DSS administration, then returned to normal after administration of DSS was stopped. In conclusion, using Msi-1 as a marker for intestinal stem/precursor cells, we could describe the behavior of intestinal stem/precursor cells during inflammation.

ACKNOWLEDGMENT

We are very grateful to Prof. H. Okano (Keio University) for providing antibody and cDNA of Msi-1.

REFERENCES

1. Renehan AG, Bach SP, Potten CS: The relevance of apoptosis for cellular homeostasis and tumorigenesis in the intestine. Can J Gastroenterol 15:166–176, 2001
2. Potten CS: Stem cells in gastrointestinal epithelium: numbers, characteristics and death. Philos Trans R Soc Lond B Biol Sci 353:821–830, 1998
3. Potten CS, Grant HK: The relationship between ionizing radiation-induced apoptosis and stem cells in the small and large intestine. Br J Cancer 78:993–1003, 1998
4. Potten CS, Martin K, Kirkwood TB: Ageing of murine small intestinal stem cells. Novartis Found Symp 235:66–84, 2001
5. Nakamura M, Okano H, Blendy JA, Montell C: Musashi, a neural RNA-binding protein required for Drosophila adult external sensory organ development. Neuron 13:67–81, 1994
6. Guo M, Jan LY, Jan YN: Control of daughter cell fates during asymmetric division: interaction of Numb and Notch. Neuron 17:27–41, 1996
7. Zeng C, Younger-Shepherd S, Jan LY, Jan YN: Delta and Serrate are redundant Notch ligands required for asymmetric cell divisions within the Drosophila sensory organ lineage. Genes Dev 12:1086–1091, 1998
8. Wang S, Younger-Shepherd S, Jan LY, Jan YN: Only a subset of the binary cell fate decisions mediated by Numb/Notch signaling in Drosophila sensory organ lineage requires Suppressor of Hairless. Development 124:4435–4446, 1997
9. Kaneko Y, Sakakibara S, Imai T, Suzuki A, Nakamura Y, Sawamoto K, Ogawa Y, Toyama Y, Miyata T, Okano H: Musashi1: an evolutionally conserved marker for CNS progenitor cells including neural stem cells. Dev Neurosci 22:139–153, 2000
10. Palm K, Salin-Nordstrom T, Levesque MF, Neuman T: Fetal and adult human CNS stem cells have similar molecular characteristics and developmental potential. Brain Res Mol Brain Res 78:192–195, 2000
11. Shu HJ, Saito T, Watanabe H, Ito JI, Takeda H, Okano H, Kawata S: Expression of the Musashi1 gene encoding the RNA-binding protein in human hepatoma cell lines. Biochem Biophys Res Commun 293:150–154, 2002
12. Kayahara T, Sawada M, Takahashi M, Fuki H, Seno H, Fukuzawa H, Suzuki K, Hiai H, Kageyama R, Okano H, Chiba T: Candidate marker for stem and early progenitor cells, Musashi-1 and Hes1, are expressed in crypt base columnar cells of mouse small intestine. FEBS Lett 535:131–135, 2003
13. Nishimura S, Wakabayashi N, Toyoda K, Kashima K, Mitsufuji S: Expression of Musashi-1 in human normal colon crypt cells, A pposible stem cell marker of human colon epithelium. Dig Dis Sci 48:1523–1529, 2003
14. Williams KL, Fuller CR, Dieleman LA, DaCosta CM, Haldeman KM, Sartor RB, Lund PK: Enhanced survival and mucosal repair after dextran sodium sulfate-induced colitis in transgenic mice that overexpress growth hormone. Gastroenterology 120:925–937, 2001
15. Good P, Yoda A, Sakakibara S, Yamamoto A, Imai T, Sawa H, Ikeuchi T, Tsuji S, Satoh H, Okano H: The human Musashi homolog 1 (MSI1) gene encoding the homologue of Musashi/Nrp-1, a neural RNA-binding protein putatively expressed in CNS stem cells and neural progenitor cells. Genomics 52:382–384, 1998
16. Sakakibara S, Imai T, Hamaguchi K, Okabe M, Aruga J, Nakajima K, Yasutomi D, Nagata T, Kurihara Y, Uesugi S, Miyata T, Ogawa M, Mikoshiba K, Okano H: Mouse-Musashi-1, a neural RNA-binding protein highly enriched in the mammalian CNS stem cell. Dev Biol 176:230–242, 1996
17. Sakakibara S, Okano H: Expression of neural RNA-binding proteins in the postnatal CNS: implications of their roles in neuronal and glial cell development. J Neurosci 17:8300–8312, 1997
18. Sakakibara S, Nakamura Y, Satoh H, Okano H: RNA-binding protein Musashi2: developmentally regulated expression in neural precursor cells and subpopulations of neurons in mammalian CNS. J Neurosci 21:8091–8107, 2001
19. Artavanis-Tsakonas S, Rand MD, Lake RJ: Notch signaling: cell fate control and signal integration in development. Science 284:770–776, 1999
20. Uemura T, Shepherd S, Ackerman L, Jan LY, Jan YN: Numb, a gene required in determination of cell fate during sensory organ formation in Drosophila embryos. Cell 58:349–360, 1989
21. Fortini ME, Artavanis-Tsakonas S: Notch: neurogenesis is only part of the picture. Cell 75:1245–1247, 1993
22. Zhong W, Feder JN, Jiang MM, Jan LY, Jan YN: Asymmetric localization of a mammalian numb homolog during mouse cortical neurogenesis. Neuron 17:43–53, 1996
23. Frise E, Knoblich JA, Younger-Shepherd S, Jan LY, Jan YN: The Drosophila Numb protein inhibits signaling of the Notch receptor during cell-cell interaction in sensory organ lineage. Proc Natl Acad Sci USA 93:11925–11932, 1996
24. Kuroda K, Tani S, Tamura K, Minoguchi S, Kurooka H, Honjo T: Delta-induced Notch signaling mediated by RBP-J inhibits MyoD expression and myogenesis. J Biol Chem 274:7238–7244, 1999

25. Zhong W, Jiang MM, Schonemann MD, Meneses JJ, Pedersen RA, Jan LY, Jan YN: Mouse numb is an essential gene involved in cortical neurogenesis. Proc Natl Acad Sci USA 97:6844–6849, 2000
26. Okabe M, Imai T, Kurusu M, Hiromi Y, Okano H: Translational repression determines a neuronal potential in Drosophila asymmetric cell division. Nature 411:94–98, 2001
27. Hirota Y, Okabe M, Imai T, Kurusu M, Yamamoto A, Miyao S, Nakamura M, Sawamoto K, Okano H: Musashi and seven in absentia downregulate Tramtrack through distinct mechanisms in Drosophila eye development. Mech Dev 87:93–101, 1999
28. Hermann GJ, Leung B, Priess JR: Left–right asymmetry in C. elegans intestine organogenesis involves a LIN–12/Notch signaling pathway. Development 127:3429–3440, 2000
29. Imai T, Tokunaga A, Yoshida T, Hashimoto M, Mikoshiba K, Weinmaster G, Nakafuku M, Okano H: The neural RNA-binding protein Musashi1 translationally regulates mammalian numb gene expression by interacting with its mRNA. Mol Cell Biol 21:3888–3900, 2001
30. Okabe M, Imai T, Kurusu M, Hiromi Y, Okano H: Translational repression determines a neuronal potential in Drosophila asymmetric cell division. Nature 411:94–98, 2001
31. Reddy GV, Rodrigues V: Sibling cell fate in the Drosophila adult external sense organ lineage is specified by prospero function, which is regulated by Numb and Notch. Development 126:2083–2092, 1999
32. Knoblich JA, Jan LY, Jan YN: Asymmetric segregation of Numb and Prospero during cell division. Nature 377:624–627, 1995
33. Doe CQ, Spana EP: A collection of cortical crescents: asymmetric protein localization in CNS precursor cells. Neuron 15:991–995, 1995
34. Paris F, Fuks Z, Kang A, Capodieci P, Juan G, Ehleiter D, Haimovitz-Friedman A, Cordon-Cardo C, Kolesnick R: Endothelial apoptosis as the primary lesion initiating intestinal radiation damage in mice. Science 293:293–297, 2001
35. Bromley M, Rew D, Becciolini A, Balzi M, Chadwick C, Hewitt D, Li YQ, Potten CS: A comparison of proliferation markers (BrdUrd, Ki-67, PCNA) determined at each cell position in the crypts of normal human colonic mucosa. Eur J Histochem 40:89–100, 1996
36. Steeb CB, Shoubridge CA, Tivey DR, Read LC: Systemic infusion of IGF-I or LR(3)IGF-I stimulates visceral organ growth and proliferation of gut tissues in suckling rats. Am J Physiol 272:G522–G533, 1997
37. Booth C, Potten CS: Effects of IL-11 on the growth of intestinal epithelial cells in vitro. Cell Prolif 28:581–594, 1995
38. Potten CS, Kellett M, Roberts SA, Rew DA, Wilson GD: Measurement of in vivo proliferation in human colorectal mucosa using bromodeoxyuridine. Gut 33:71–78, 1992
39. Potten CS, Loeffler M: Stem cells: attributes, cycles, spirals, pitfalls and uncertainties. Lessons for and from the crypt. Development 110:1001–1020, 1990
40. Garabedian EM, Roberts LJ, McNevin MS, Gordon JI: Examining the role of Paneth cells in the small intestine by lineage ablation in transgenic mice. J Biol Chem 272:23729–23740, 1997
41. Merritt AJ, Potten CS, Kemp CJ, Hickman JA, Balmain A, Lane DP, Hall PA: The role of p53 in spontaneous and radiation-induced apoptosis in the gastrointestinal tract of normal and p53–deficient mice. Cancer Res 54:614–617, 1994
42. Bach SP, Renehan AG, Potten CS: Stem cells: the intestinal stem cell as a paradigm. Carcinogenesis 21:469–476, 2000
43. Griffiths DF, Davies SJ, Williams D, Williams GT, Williams ED: Demonstration of somatic mutation and colonic crypt clonality by X—linked enzyme histochemistry. Nature 333:461–463, 1988
44. Kuraguchi M, Cook H, Williams ED, Thomas GA: Differences in susceptibility to colonic stem cell somatic mutation in three strains of mice. J Pathol 193:517–521, 2001
45. Toyoda K, Nishikawa A, Furukawa F, Kawanishi T, Hayashi Y, Takahashi M: Cell proliferation induced by laxatives and related compounds in the rat intestine. Cancer Lett 83:43–49, 1994
46. Potten CS, O'Shea JA, Farrell CL, Rex K, Booth C: The effects of repeated doses of keratinocyte growth factor on cell proliferation in the cellular hierarchy of the crypts of the murine small intestine. Cell Growth Differ 12:265–275, 2001
47. Martin K, Kirkwood TB, Potten CS: Age changes in stem cells of murine small intestinal crypts. Exp Cell Res 241:316–323, 1998
48. Paulus U, Potten CS, Loeffler M: A model of the control of cellular regeneration in the intestinal crypt after perturbation based solely on local stem cell regulation. Cell Prolif 25:559–578, 1992
49. Kozoni V, Tsioulias G, Shiff S, Rigas B: The effect of lithocholic acid on proliferation and apoptosis during the early stages of colon carcinogenesis: differential effect on apoptosis in the presence of a colon carcinogen. Carcinogenesis 21:999–1005, 2000
50. Colussi C, Fiumicino S, Giuliani A, Rosini S, Musiani P, Macri C, Potten CS, Crescenzi M, Bignami M: 1,2-Dimethylhydrazine-induced colon carcinoma and lymphoma in msh2(–/–) mice. J Natl Cancer Inst 93:1534–1540, 2001
51. Potten CS, Li YQ, O'Connor PJ, Winton DJ: A possible explanation for the differential cancer incidence in the intestine, based on distribution of the cytotoxic effects of carcinogens in the murine large bowel. Carcinogenesis 13:2305–2312, 1992